Sorting of Double-Walled Carbon Nanotubes According to Their Outer Wall Electronic Type *via* a Gel Permeation Method

Katherine E. Moore,[†,‡] Moritz Pfohl,[‡,§] Daniel D. Tune,[†,‡] Frank Hennrich,[‡] Simone Dehm,[‡] Venkata Sai K. Chakradhanula,[‡,⊥] Christian Kübel,[‡,⊥,∥] Ralph Krupke,[‡,§] and Benjamin S. Flavel[*,‡]

[†]Centre for Nanoscale Science and Technology, School of Chemical and Physical Sciences, Flinders University, Adelaide 5042, Australia, [‡]Institute of Nanotechnology, Karlsruhe Institute of Technology, 76021 Karlsruhe, Germany, [§]Institute for Materials Science, Technische Universität Darmstadt, 64287 Darmstadt, Germany, [⊥]Helmholtz Institute Ulm Electrochemical Energy Storage, 89081 Ulm, Germany, and [∥]Karlsruhe Nano Micro Facility, Karlsruhe Institute of Technology, 76021 Karlsruhe, Germany

ABSTRACT In this work, we demonstrate the application of the gel permeation technique to the sorting of double-walled carbon nanotubes (DWCNTs) according to their outer wall electronic type. Our method uses Sephacryl S-200 gel and yields sorted fractions of DWCNTs with impurities removed and highly enriched in nanotubes with either metallic (M) or semiconducting (S) outer walls. The prepared fractions are fully characterized using optical absorption spectroscopy, transmission electron microscopy, and atomic force microscopy, and the entire procedure is monitored in real time using process Raman analysis. The sorted DWCNTs are then integrated into single nanotube field effect transistors, allowing detailed electronic measurement of the transconductance properties of the four unique inner@outer wall combinations of S@S, S@M, M@S, and M@M.

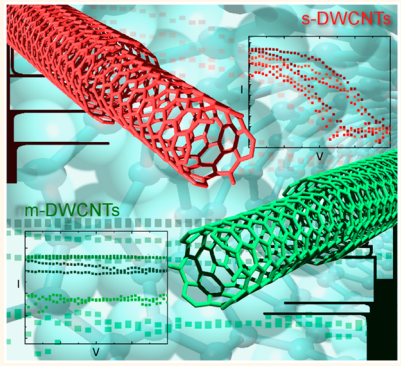

KEYWORDS: carbon nanotube · double · separation · electronic character · sorting · purification · Sephacryl gel

From an applications viewpoint, double-walled carbon nanotubes (DWCNTs) have long been idealized as candidates for use in nanotube-based sensor devices where it is proposed that the outer wall can be functionalized, leaving the inner wall pristine and available for signal transduction. For example, Wang *et al.* treated DWCNTs with concentrated acid mixtures, confirmed that functionalization was mostly limited to the outer wall,[1] then extended that work to show that diazonium-modified DWCNTs retained 33 times more current-carrying capacity than similarly functionalized SWCNTs when integrated into thin films.[2] Later, the same group used chemically modified DWCNT field effect transistors (FETs) for the detection of amines, observing 6000 times higher chemical selectivity for amine-containing analytes compared to other small molecules,[3] demonstrating that DWCNT FETs can achieve ultrahigh detection sensitivity (~1 ppb) with the added advantages of increased selectivity and reduced occurrence of nonspecific binding.

From a fundamental viewpoint, DWCNTs represent the simplest form of a multi-walled carbon nanotube (MWCNT), which makes them ideal candidates for investigating the effects of the interwall coupling between component nanotubes, which can produce some remarkable and unexpected phenomena. For example, Okada and Oshiyama calculated that due to overlap of the electronic states of the constituent nanotubes, some S@S DWCNTs can behave entirely as metals,[4] while Moradian *et al.* calculated that in some mixed-wall DWCNTs the two walls can even exchange electronic type.[5] Such predictions have further drawn the attention of experimentalists to investigate the properties of DWCNTs through the use of FETs, notably Liu *et al.*[6] and Bouilly *et al.*,[7] who have provided unique insights into

* Address correspondence to benjamin.flavel@kit.edu.

Received for review December 2, 2014 and accepted March 10, 2015.

Published online March 10, 2015
10.1021/nn506869h

the transconductance properties of the different inner@outer wall combinations of DWCNTs. Spectroelectrochemistry has also been employed by Kalbac *et al.* to investigate the effects of charge transfer between the four DWCNT combinations, where the required shift in Fermi level to achieve charge transfer from outer to inner wall was found to increase in the order of M@M < S@M < M@S < S@S.[8]

Notwithstanding the aforementioned studies, the use of DWCNTs has remained relatively limited despite their clear potential. This is in part due to DWCNTs suffering many of the same setbacks initially experienced by SWCNTs, in particular, the lack of a method to synthesize pure, electronically well-defined raw material. For this reason, several groups are focusing on the subsequent processing and sorting of DWCNT raw material. While sorting by inner wall type remains elusive, the relatively small field of DWCNT sorting has already seen density gradient ultracentrifugation (DGU) used in the removal of large and small diameter SWCNT contaminants[9] as well as DWCNT separation by length[10] and outer wall electronic type.[11] However, the use of Sephacryl gel chromatography has remained notably underutilized in the processing of DWCNTs. In the case of SWCNTs, the technique has allowed for the high-throughput separation of metallic from semiconducting species and in some cases can also enrich zigzag and (*n*, 0) species.[12] The works of Kataura and co-workers,[13,14] Strano and co-workers,[15,16] and our group[17,18] have further developed the technique to afford highly (n,m) pure SWCNT suspensions. In the field of DWCNT sorting, we recently demonstrated the use of Sephacryl gel to purify raw DWCNT material by removing SWCNT contaminants.[19] Based on the already proven success of Sephacryl gel for the separation of SWCNTs by electronic type, we anticipated that perhaps such an approach may also offer an avenue for the separation of DWCNTs. Although the ultimate goal remains the preparation of DWCNTs with both defined outer and inner walls, this current work makes a significant advance in that direction by providing a high-throughput method to prepare DWCNTs with defined outer wall electronic type.

The literature contains several examples of the electronic separation of large diameter arc-discharge (AD) SWCNTs by a cosurfactant gel separation. Miyata *et al.*,[20] Wu *et al.*[21] and Zhang *et al.*[22] have all demonstrated the use of cosurfactant separation for large diameter SWCNTs using sodium dodecyl sulfate (SDS) and sodium cholate (SC), and on the basis of these reports, a similar cosurfactant approach would intuitively appear to be applicable to DWCNTs with their relatively large outer walls. It is this method that we now describe.

RESULTS AND DISCUSSION

Raw DWCNTs suspended with SC were applied to a gel bed under SDS and washed through with further SDS solution, and the "flow-through" material was collected. Time-lapse photography (Figure S1 of the Supporting Information) shows that separation begins to occur rapidly with the formation of four bands of differing concentration and color. Over time, each band spreads out and is subsequently eluted at a different time. To follow this process, we monitored the composition of the eluted liquid using a process Raman analyzer, or "process Raman", where the integrated G-band intensity is plotted against time and is shown in Figure 1a. For comparison, the same process was repeated for large diameter AD SWCNTs and small diameter HiPco SWCNTs (see Figures S2 and S3, Supporting Information, for more information). For the DWCNT material, four bands were eluted at 7, 10, 18, and 20 min, respectively. The eluted material corresponding to each peak in the process Raman data was then measured using optical absorption spectroscopy (Figure S4, Supporting Information).

Bands 1 and 2 exhibit very similar optical properties, with two broad peaks at 695 and 750 nm and a series of peaks between 1030 and 1215 nm (the spectrum of band 2 can be seen in Figure 1b). These absorption regimes correspond to M_{11} transitions of large diameter (~1.3−1.6 nm) metallic (m-) nanotube walls[23] and to the S_{11} transitions of smaller diameter (~0.7−0.9 nm) semiconducting (s-) nanotube walls[24] or S_{22} transitions of large diameter s-nanotubes, respectively. Considering that the difference between these two diameter distributions is ~0.6−0.8 nm, and knowing that the interwall spacing varies between 0.33 and 0.41 nm,[25] it is therefore likely that these peaks correspond to the inner- and outer-wall pairs of DWCNTs. In the case of band 1, there is additional broadness between 1030 and 1215 nm suggesting that there are other large-diameter s-nanotubes present. Furthermore, the large background and low peak intensity suggest that these nanotubes have poor optical properties and are most likely defected. The absorption spectrum of band 2 is, however, in good agreement with that previously reported by Green and Hersam for metallic outer-wall-enriched DWCNTs,[11] and it is this fraction that we assign to be metallic outer walled DWCNTs (m-DWCNTs) and these are used in further experiments.

The absorption measurement of band 3 (seen in Figure 1c) is significantly different from that of either band 1 or band 2. There is a large, broad feature centered at ~1050 nm consisting of a multitude of peaks, with a series of smaller peaks between 400 and 600 nm. These peaks correspond to the S_{22} transitions of large diameter nanotubes (~1.5−1.6 nm), S_{11} transitions of small diameter nanotubes (~0.7−1 nm), and S_{33} transitions of large diameter semiconducting nanotubes, respectively. Importantly, there is a clear absence of peaks in the range of 600−800 nm; the region where large diameter M_{11} peaks were observed for bands 1 and 2. Again, this spectrum is in agreement

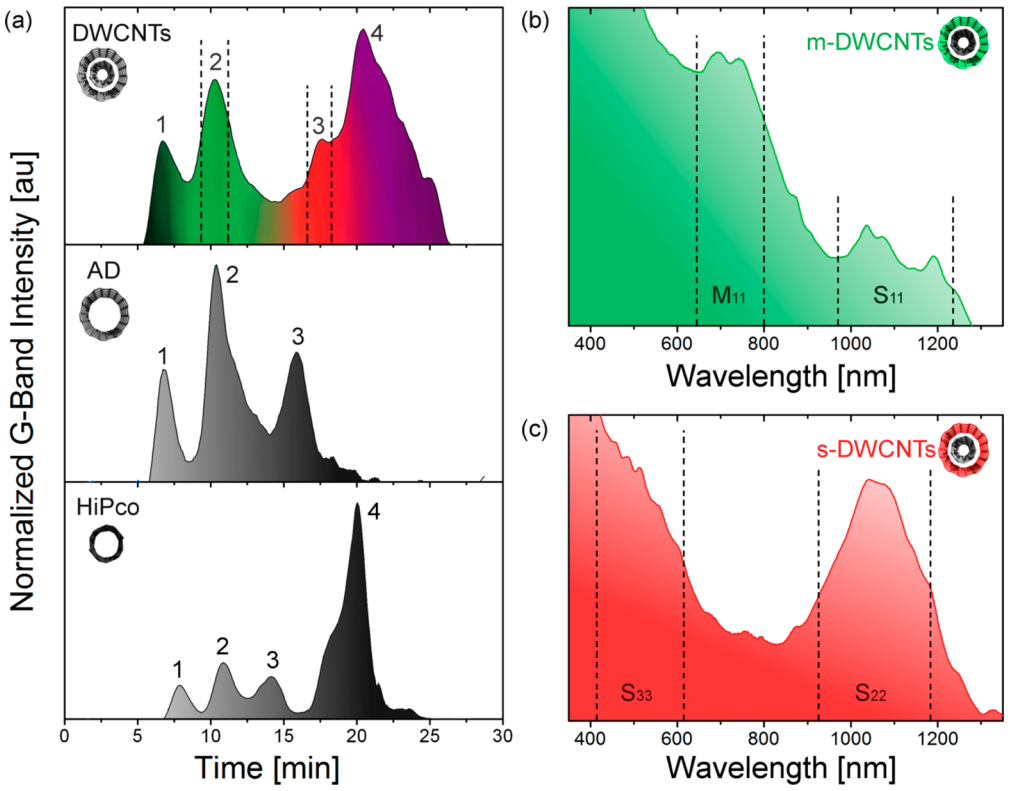

Figure 1. Cosurfactant separation of DWCNTs *via* gel permeation. (a) Elution profiles of the normalized G-band Raman mode intensity for DWCNTs, AD SWCNTs, and HiPco SWCNTs. The dashed lines in the DWCNT elution profile highlight bands 2 and 3, which from the absorption spectra, seen in (b) and (c), correspond to DWCNTs with metallic and semiconducting outer walls. Regions of S_{ii} and M_{ii} transitions are highlighted in each spectrum.

with the literature[11] and indicates that the vast majority of the large diameter nanotubes present are semiconducting in nature. Therefore, band 3 was assigned as semiconducting outer wall DWCNTs (s-DWCNTs) and this material was used for subsequent experiments.

Interestingly, the three bands observed in the AD SWCNT (1.3−1.7 nm) separation occur at approximately the same time as the first three bands of the DWCNT material (7, 10, and 16 min). Comparison of the absorption measurements of the three bands (Figure S2, Supporting Information) with those of the DWCNT material reveals that the AD SWCNTs undergo the same separation process, *i.e.*, defected material followed by metallic and then semiconducting nanotubes. However, despite the semiconducting fraction (band 3) exhibiting equally high purity as the s-DWCNTs, the metallic fraction (band 2) shows a large S_{22} feature, indicating the presence of many s-nanotubes. Thus, the cosurfactant gel separation is not as effective for metallic large diameter nanotubes as it is for DWCNTs, despite having the same mean diameter. While they are expected to be the same in terms of the surface properties, such as surfactant wrapping, it is important not to discount the presence of an inner wall, which will introduce an increased stiffness to the DWCNT and influence its permeation through the gel. Furthermore, the possibility for interwall coupling may provide an influence on the overall electronic properties of the DWCNT and its wrapping by SDS. These subtle differences may explain the difference between AD and DWCNT separation.

Lastly, band 4 (Figure S4, Supporting Information) shows peaks in the range of 1050−1250 nm and less intense, broader peaks between 600 and 800 nm. These are indicative of S_{11} and S_{22} transitions of small diameter SWCNTs, respectively, and are in agreement with our previous work, which also saw the SWCNTs eluted last from the column, despite the significantly different surfactant conditions used.[19] It can be seen that band 4 aligns well with the bulk of the HiPco "flow-through" material eluted at 20 min also. Interestingly, the HiPco SWCNTs also experience some degree of electronic sorting, with the first three peaks exhibiting M_{11} features (Figure S2, Supporting Information).

Comparing band 2 for all materials; it seems possible that the m-DWCNT fraction may contain large and small diameter m-SWCNTs. Likewise for band 3, the s-DWCNT fraction may contain large diameter s-SWCNTs and small diameter m-SWCNTs. However, as the concentration of these "contaminant" species is low in the raw material (<30%), their overall contribution to the m- and s-DWCNT fractions is likely to be similarly low and this is supported by TEM analysis, as discussed later. Additional characterization by Raman spectroscopy of nanotube films can be found in Figure S5 of the Supporting Information.

While Figure 1a shows well-isolated metallic and semiconducting bands, the route toward successful separation was not as straightforward as it at first appeared it might be. In light of previously reported diameter- and SDS concentration-dependent adsorption of small diameter SWCNTs[13,18,26] and our previous work on DWCNTs,[19] it was proposed that the preparation of m-DWCNTs may be as simple as sequentially reducing the SDS concentration until the flow-through material consisted only of m-DWCNTs. This approach was systematically investigated and was ultimately unsuccessful (see Figure S6 (a), Supporting Information). This suggests that SDS on its own does not exhibit any sensitivity toward electronic character for DWCNTs. Similarly, a separation in SC alone does not yield any enrichment by diameter or electronic type, as seen in our previous work.[19]

As previous reports in the literature for SWCNT sorting *via* gel permeation have demonstrated a high dependence upon surfactant encapsulation,[13,15] it therefore follows that the separation of DWCNTs is similar. The interaction between surfactant and nanotubes has been extensively investigated and reveals that different surfactant conformations (random, hemimicelle or cylindrical micelle) arise depending on nanotube diameter and the surfactant concentration of its environment.[27−29] For example, SDS wrapping of small diameter nanotubes (<1 nm) tends to result in a highly disordered random configuration at low SDS concentrations (packing densities of ∼1.0 molecules nm^{-2})[28,30] and more ordered, cylindrical wrapping at high SDS concentrations (2.8 molecules nm^{-2}).[28] The wrapping of large diameters (>1 nm) is also disordered at low concentration but forms hemimicelles at high SDS concentration.[28,30] Furthermore, the extent of SDS encapsulation is also dependent upon electronic character with metallic nanotubes having a higher degree of SDS wrapping than semiconducting nanotubes, owing to the increased polarizability.[31] These different surfactant conformations are responsible for the nanotubes' interaction with the gel environment with lower wrapping densities causing a stronger interaction. Thus, in the low concentration regime, semiconducting nanotubes (with disordered surfactant encapsulation layers for both large and small diameters) are adsorbed to the gel, while metallic nanotubes experience no interaction.[13,15,26]

Although the correct mechanism of the cosurfactant separation remains speculative, we now present a possible mechanism based on the current understanding of SDS encapsulation mentioned above and reported SDS-based gel separations.[13,15,26]

Upon initial addition to a gel column under SDS, the nanotubes are entirely wrapped in SC and experience limited interaction with the gel. As they traverse the gel, a surfactant exchange process begins and an initial separation occurs. This separation is enhanced by washing with additional SDS, which results in nanotubes that are either partially or completely wrapped in SDS. As metallic nanotubes are known to have a stronger interaction with SDS compared to semiconducting nanotubes,[31] they may become more fully wrapped. In which case, the metallic nanotubes would continue to have a limited interaction with the gel as they traverse the column, as is commonly seen in SWCNT separations.[13,15,26] Consequently, the m-DWCNTs elute first from the gel.

From experiments with the raw material at 0.5 wt % SDS (see Figure S6 (a), Supporting Information), it is also clear that even at low SDS concentrations it is not possible to have a sufficiently low or disordered wrapping of SDS on the s-DWCNTs to facilitate a strong interaction with the gel. Nonetheless, due to the well-known electronic sensitivity of SDS,[11,13,31,32] it is expected that the interchange of SC with SDS occurs more readily on m-DWCNTs compared to s-DWCNTs. Likewise, the increased curvature of small diameter SWCNTs is expected to make it more difficult for SC to be exchanged with SDS. Consequently, as seen in the elution profile (Figure 1), bands of s-DWCNTs and SWCNTs form.

While Figure 1 demonstrates separation under optimized conditions (1 wt % SDS: 1 wt % SC), several other surfactant ratios and concentrations where also employed. In the case of a low SDS concentration on the column (0.5 wt %) and high relative SC concentration in solution (1 wt %), it is possible that the SDS concentration is too low to displace the SC from the nanotube sidewalls. Alternatively, for a high SDS concentration on the column (2 wt %) and a low relative SC concentration in solution (1 wt %), the SDS is quickly able to displace the SC and form stable hemispheres around the nanotube, limiting the interaction with the gel. In both cases the raw material remains together as one band, as seen in Figure S7 (b) and (c) (Supporting Information). When keeping the surfactant ratio the same (1:1), but increasing the concentration (2 wt %), the resolution of separation is also reduced, as seen in Figure S7 (d) (Supporting Information). This in line with previous computational work,[27,28] as well as experimental work of Kataura and co-workers,[13] Strano and co-workers,[15] Blanch *et al.*,[26] and our work,[17,18] where high concentrations of SDS in general reduce the interaction of nanotubes with the gel.

The proposed mechanism may also explain why taking enriched DWCNTs from our previous method,[19] which were separation from a mixture of SWCNTs and DWCNTs, is unsuccessful for subsequent separation according to outer wall electronic character (see Figure S6 (b) (Supporting Information) for more information). In our previous work, the DWCNTs were suspended in 2 wt % SDS and added to a gel column under 2 wt % SDS. Only a very small amount of the overall nanotube population became adsorbed to the gel, presumably

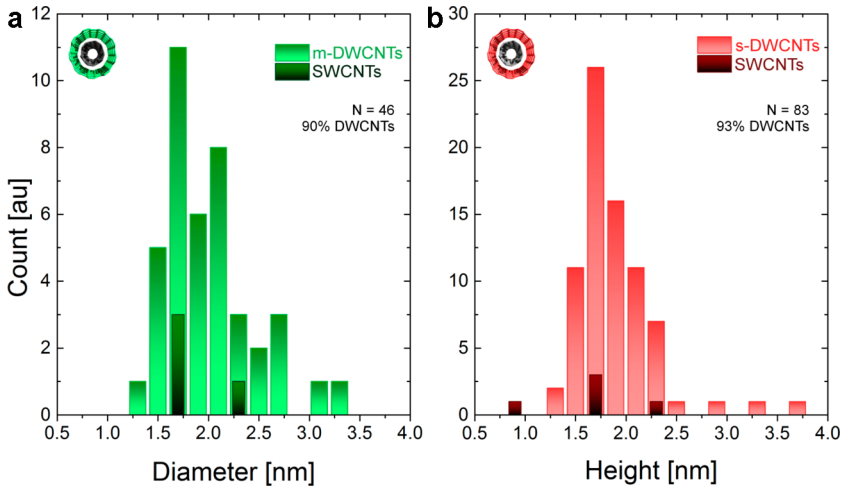

Figure 2. TEM analysis of the sorted DWCNTs with (a) metallic and (b) semiconducting outer walls, where diameter distributions can be seen for DWCNTs, SWCNTs, and MWCNTs. The sample number and resultant DWCNT purity are given in each case.

only those with a sufficiently low SDS coverage to facilitate an interaction with the gel. These adsorbed nanotubes were then washed off with 1 wt % SC, which is exactly the same surfactant and concentration used for starting material in the current work. Thus, it should follow that enriched DWCNTs obtained from the previous method can be further separated by electronic character using the method described in this work. However, no electronic separation of this material is observed. We attribute this to the fact that our proposed mechanism is reliant upon having DWCNTs with a strong tendency to be wrapped by both SDS and SC because our separation method is reliant on the intermixing of SC with SDS on the nanotube surface, but these nanotubes are not those that result from the previous method. In the previous method the use of a high SDS concentration yields only those nanotubes with a weak preference for SDS wrapping. Hence, the appropriate interchange/intermixing of surfactants exploited in the current work is simply overwhelmed by a stronger tendency to be wrapped with SC. Nevertheless, the current method also separates DWCNTs from SWCNTs (as seen in Figure 1 and Figure S4, Supporting Information), which makes a preliminary separation of DWCNTs from SWCNTs unnecessary.

To estimate the DWCNT purity as well as the electronic purity of m-DWCNT and s-DWCNT fractions, transmission electron microscopy (TEM), absorption spectroscopy, and atomic force microscopy (AFM) were employed. TEM histograms of diameter distributions of DWCNTs and SWCNTs are presented in Figure 2 with representative TEM micrographs for all separated fractions seen in Figures S8−S11 (Supporting Information). For the metallic enriched DWCNTs, it can be seen that the sample predominantly consists of DWCNTs with a purity of 90%, with very few SWCNTs present. This is in agreement with the absorption spectra, in which small diameter nanotubes in any significant amount cannot be identified. Furthermore, the TEM shows an average DWCNT diameter of ∼1.7 nm, in agreement with that obtained previously for metallic DWCNTs sorted form the same starting material.[11] TEM analysis of the semiconducting enriched fraction reveals a similar DWCNT purity of 93% and an average diameter of ∼1.6 nm. A negligible number of MWCNTs were observed (<2 in each sample) and TEM failed to reveal the presence of any other carbon structures such as nanoribbons. However, owing to the limitations associated with sample size in TEM analysis, we are unable to definitely discount the presence of either.

Despite AFM and TEM being established methods for nanotube characterization, it should be noted that a new approach has been recently reported by Kominkova *et al.*, which is capable of discerning the ratio of SWCNTs:DWCNTs, although it requires a spectroelectrochemical cell.[33] Due to the fact that TEM confirms that the samples contain predominantly DWCNTs, reasonable estimates of electronic purity can be obtained from the absorption spectroscopy measurements,[11] where the contributions from SWCNTs are thus assumed to be negligible. By measuring the absorption profile of nanotube films before and after treatment with thionyl chloride, which depletes S_{11} (and some S_{22}) transitions of the outer walls,[9,11,19] peak areas for metallic and semiconducting outer wall species can be calculated. These can then be compared to those of AD SWCNTs, which have a known composition of 1:2 metallic/semiconducting (see Figures S12 and S13, Supporting Information, for more information). This yields purities of ∼90% and ∼70% for semiconducting and metallic enriched DWCNTs, respectively, which is comparable to that achieved by Green and Hersam using DGU (96% and 98% respectively).[11] This compliments the existing literature on SWCNT sorting, where DGU[34−37] and gel-based

sorting methods[12,13,15,18] have consistently proven to be the preferred techniques to achieve high purity carbon nanotube solutions.

While TEM and absorption spectroscopy are the accepted characterization methods for purity of enriched DWCNT material,[11] we have also included AFM measurements as it is a common method used to estimate diameter distributions. AFM samples were prepared by spin coating of nanotube suspensions onto silicon oxide surfaces. Representative AFM images can be seen in Figure S14 (Supporting Information) with diameter and length distributions seen in Figures S15−S17 (Supporting Information). While the measured average diameters of the m-DWCNT and s-DWCNT (1.61 ± 0.14 nm and 1.56 ± 0.04 nm, respectively) are in agreement with TEM there is a significant discrepancy regarding the number of small diameter nanotubes, which can only correspond to SWCNTs. This unexpectedly high proportion of small diameter nanotubes is also seen here in the case of large diameter AD SWCNTs. These have a diameter range of 1.3−1.7 nm, but the AFM shows that 25% of the AD nanotubes have diameters of 1 nm or less. This anomalous result raises questions about sample preparation; where the different surfactant wrapping of small and large diameter nanotubes may give rise to different degrees of bundling or adhesion during the spin-coating process. This could potentially generate a situation in which there is bias toward more of the small diameter nanotubes being individually present on the surface than in the real solution. Of course, this skews the statistical analysis toward smaller diameters because only those nanotubes that are individually dispersed on the surface are counted. This highlights the difficulty associated with correctly assessing the composition of carbon nanotube suspensions.

While AFM may suffer from problems associated with sample preparation, TEM and absorption spectroscopy also present challenges in characterization. TEM is the definitive tool for the conclusive identification of DWCNTs and provides quantitative characterization of the diameter distribution, yet it only samples a small proportion of the entire nanotube population. On the other hand, while absorption measurements probe the entire nanotube population, the interpretation of the resulting spectra is difficult due to convolution of the inner and outer wall optical transitions. This can be somewhat overcome by bleaching the optical transitions of the outer walls through doping, however in practice chemical shielding of the inner wall by its corresponding outer wall is not complete.[8] This also requires nanotubes to be in thin film form, which gives rise to large scattering backgrounds and red-shifting of the peak positions.[32,38−40] Although comparing M_{11} and S_{11} peak areas of sorted DWCNT material to those of the AD SWCNTs provides the best avenue for spectroscopic determination of purity at this time, it does not consider the differing absorption cross sections of the various nanotube species and is, thus, an estimate. In an attempt to improve the purity of the separated m- and s-DWCNT fractions, a subsequent separation step was also conducted. However, while it somewhat improved the purity of the s-DWCNT fraction, it made little overall difference to the purity of the m-DWCNT fraction (Figures S18 and S19, Supporting Information).

The fabrication of DWCNT FETs allows for a more thorough investigation of the electronic properties than can be obtained from a purely spectroscopic analysis. Previous work has employed top contact formation *via* metal deposition onto a substrate-bound nanotube, with the character of the contacting nanotube determined postfabrication.[6,7] However, in this work we use an already established technique for nanotube device fabrication−electrophoretic deposition,[41−43] which has been demonstrated on multiple occasions to afford highly aligned single nanotube contacts.[44,45] Owing to the greater polarizability of metallic SWCNTs they are preferentially deposited over their semiconducting counterparts during the electrophoretic deposition process, which makes it difficult to selectively deposit semiconducting nanotubes from a mixture of nanotube types.[41] With the addition of a second wall this becomes practically impossible, and thus high-purity s-DWCNTs suspensions are required.

DWCNT FETs were manufactured using electron-beam lithography, metal sputtering, and lift-off, followed by electrophoretic deposition from either a m- or s-DWCNT suspension. Both AFM and scanning electron microscopy (SEM) were then used to verify the presence of only a single nanotube per device as shown in Figure 3 as well as Figure S20 (Supporting Information). It should be noted that in order to definitively determine the inner@outer wall identity of each DWCNT either Raman or TEM would be required. However, as in the work of Liu *et al.*,[6] TEM measurements require a window in the substrate in order to free-suspend the nanotube and Raman would require a confocal microscope with a diffraction limited spot and enough available excitation wavelengths to excite all combinations of inner and outer wall. As neither of these approaches were available to us, our assignment of inner@outer wall is based on previous literature examples, in which this additional characterization was possible.[6,7] The first type of behavior seen for m-DWCNTs is shown in Figure 3a, where an entirely metallic behavior is seen, with no current modulation and an increasing current (I_s) with increasing source-drain voltage (V_s). The I_s, measured in the on state at $V_s = 1$ V, was $\sim 2.3 \times 10^{-5}$ A with a calculated on/off ratio of 1.0. Although TEM of the DWCNT is the only way to conclusively confirm the identity of the inner and outer walls, as in Liu *et al.*,[6] this would require a specialized substrate and very long nanotubes. However, when

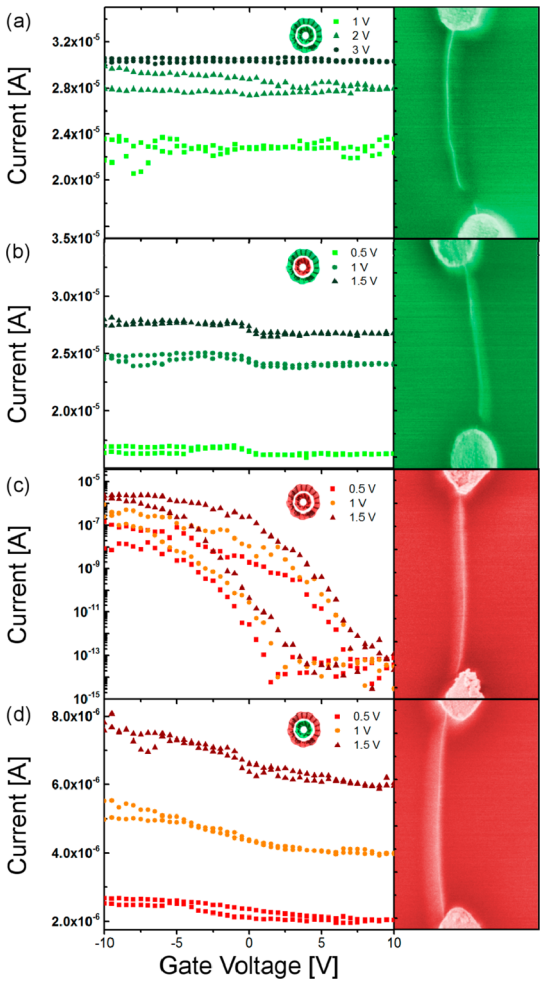

Figure 3. Transconductance measurements and corresponding false color SEM images of the four possible types of DWCNT FET: (a) M@M, (b) S@M, (c) S@S, and (d) M@S.

compared in conjunction with the spectroscopic analysis to accounts from the literature in which TEM was performed,[6,7] the transconductance measurements are a strong indicator of the presence of an M@M DWCNT.

The second type of behavior observed for metallic outer wall DWCNTs is shown in Figure 3b. Similarly to the M@M case in Figure 3a, a constant source−drain current is seen with varying gate voltage, with the exception of a slight modulation around $V_g = 0$ V. I_s in the "on-state" at $V_s = 1$ V was measured to be 2.5×10^{-5} A with an on/off ratio close to unity. This behavior is attributed to a S@M DWCNT and is in agreement with Bouilly *et al.*,[7] who also observed no modulation (on the logarithmic scale) for pristine S@M DWCNTs.

Parts c and d of Figure 3 display the two types of behavior found for devices fabricated using the s-DWCNT suspension. Figure 3c shows a very different behavior compared to that observed in the other three cases, with an on/off ratio of $\sim 10^8$ and an I_s in the on state of 3.8×10^{-7} A at $V_s = 1$ V. This strongly semiconducting behavior is assigned to an S@S DWCNT in agreement with the work of Liu *et al.*[6] and Bouilly *et al.*[7]

According to the previously reported literature, the presence of a significant band gap may result from either a large interwall spacing, a lack of $\sigma-\pi$ rehybridization owing to large diameter inner walls, or curvature differences between the inner and outer walls.[4] Without TEM, the (*n*,*m*) indices of the inner and outer walls cannot be known precisely, and hence, any conclusions about the curvature difference and inner wall rehybridization could only be speculative. However, from the TEM and AFM data, the average interwall distance for s-DWCNTs was determined to be 0.38 ± 0.15 nm and the outer wall diameter of the measured DWCNT is 1.54 nm. TEM analysis of interwall distance for all DWCNT fractions can be found in Figure S21 (Supporting Information). Moradian *et al.*[5] modeled various commensurate DWCNTs (*i.e.*, where the ratio between the unit cell lengths of the two walls is a rational number) with the (20,0) outer wall, which has a diameter of 1.566 nm similar to that observed here. When an (8,0) nanotube was inserted as the inner wall (diameter = 0.626 nm), the DWCNT remained semiconducting with an interwall distance of 0.47 nm. If the inner wall is replaced by a (10,0) nanotube (diameter = 0.783 nm), the interwall distance is reduced to 0.3915 nm and the DWCNT becomes metallic in nature. Because the average interwall distance measured here is less than that presented by Moradian *et al.*, but the nanotube remains semiconducting, it is therefore likely that the observed semiconducting behavior is due to the S@S DWCNT being incommensurate.

The last remaining DWCNT combination is M@S, shown in Figure 3d. A slight current modulation is observed with an on/off ratio of 1.4 (marginally higher than M@M or S@M) and an on-state current of $I_s = 5.5 \times 10^{-6}$ A at $V_s = 1$ V. In this instance, the current is carried predominately by the inner metallic wall, with the large semiconducting outer wall being gateable. This behavior differs from that observed by Bouilly *et al.*,[7] who were unable to differentiate between M@M and M@S DWCNTs. The authors attributed this to the difficulty in determining the nature of the outer wall due to the constant current flowing thought the metallic inner wall. Of course, that problem is resolved in our work because the observation of current modulation can be coupled to the fact that the nanotube was deposited from a suspension of purified s-DWCNT material, clearly allowing the behavior to be attributed to an M@S device. This is also in agreement with the work of Liu *et al.*[6] who observed clear differences in behavior between the M@M and M@S DWCNT combinations.

CONCLUSION

In this work, we present a straightforward and scalable cosurfactant column chromatography technique to produce DWCNTs with defined outer wall electronic character. The enriched DWCNTs fractions were characterized with TEM, AFM, and absorption

spectroscopy, and the time evolution of the sorting process was measured with process Raman analysis. Integration of the resultant sorted material into DWCNT field effect transistors *via* electrophoretic deposition has allowed detailed electronic measures of the nanotube characteristics to be made. In addition, correlation of the device's transconductance properties with precise knowledge of the composition of the starting solutions has allowed for accurate differentiation between the four unique inner@outer wall combinations of M@M, S@M, S@S, and M@S. We anticipate that the high throughput and relative simplicity of this approach will spur further interest into the investigation of the complex and intriguing interwall interactions of DWCNTs, as well as opening up the potential for exploiting such interactions in advanced sensor devices and other applications.

EXPERIMENTAL SECTION

The DWCNT raw material (average diameter ~2 nm) used in this work was supplied by Unidym (lot no. OE-130807). AD SWCNT raw material was obtained from Carbon Solutions (lot no. AP-387), and HiPco SWCNT raw material was obtained from NanoIntegris (lot no. R1-901). Raw nanotube starting material was prepared by suspending nanotube powder (50 mg) in aqueous SC (1 wt %, 125 mL, Sigma-Aldrich) using a tip sonicator (Weber Ultrasonics, 35 kHz, 500 W in continuous mode, 1 h, ~ 20% power). During sonication, the suspension was placed in a water bath (15 °C).

Gel filtration was performed as previously described[19] with only a few changes, using Sephacryl S-200 gel filtration medium (Amersham Biosciences) in a glass column (45 cm in length and 2 cm inner diameter). The column was filled with filtration medium (90 mL) and compacted slightly by applying pressure with compressed air to yield the desired gel height (~20 cm). The column was prepared for separation by washing with aqueous SDS (1 wt %, ~180 mL, Merk KGaA). For the separation, as-prepared nanotube suspension (~10 mL) was added to the top of the column. Once the nanotube material had completely entered the gel, the column was filled with a solution of aqueous SDS (1 wt %) under applied pressure to ensure a constant flow rate (~1 mL min^{-1}). The nanotubes were separated and the eluent was collected in fractions (~2 mL) for characterization.

Raman intensity was monitored in real-time with a Raman RXN Systems analyzer (Kaiser Optical Systems) fitted to the end of the column with an excitation wavelength of 785 nm.

Spectroscopic characterization of the sorted material was carried out by absorption spectroscopy. Absorption spectra of the sorted fractions were recorded on a Varian Cary 500 spectrophotometer.

Nanotube suspensions (10 μL) were spin-coated (1 min, 1500 rpm) onto clean silicon oxide surfaces (1 cm^2, ABC GmbH) and then gently rinsed with water. To measure nanotube lengths and heights, tapping mode AFM images were taken in ambient conditions with a multimode head and a NanoScope III controller (Digital Instruments) using silicon cantilevers (resonance frequency 250−400 kHz Mikromasch). Topographic height and phase images were obtained simultaneously with feedback controls optimized for each sample.

TEM samples were prepared by drop-casting aqueous suspensions of the nanotubes onto lacey carbon coated copper grids (Quantifoil GmbH) which were then placed in a drybox (silica gel). Subsequently, samples were washed four times with water and dried similarly. TEM analysis was performed using an aberration-corrected FEI Titan 80−300 microscope operated at 300 kV and equipped with a Gatan US1000 CCD camera for imaging and electron diffraction. All micrographs were obtained with a 2K × 2K CCD camera and analyzed using the Digital Micrographs software package (Version 1.71.38, Gatan Co.).

Boron-doped p-type silicon (0.005−0.001 Ω cm, 325 μm thickness, CZ, ⟨100⟩, ABC GmbH) with a thermally grown oxide (800 nm) was used in the fabrication of FETs for electronic characterization of the nanotubes. Pd source, drain, and gate electrodes, all with a Ti adhesion layer, were fabricated by electron-beam lithography, metal sputtering, and lift off. To deposit single nanotubes between source and drain contacts, a small volume (~7 μL) of nanotube suspension (diluted 1000× with water) was placed on top of the substrate and an RF signal (ω_d = 300 kHz, V_{pp} = 2 V) was applied between the source and gate electrodes. After a short period (~1 min) the substrate was rinsed five times each with water and methanol before drying with nitrogen, and then the generator was switched off. Electronic measurements were obtained using an Agilent 4155C semiconductor parameter analyzer.

Both SEM and AFM were employed to allow selection of only those devices that consisted of a single nanotube connection. A Zeiss Gemini with 1.00 kV EHT, 2.1 mm WD, aperture size of 20 μm, and magnification of 50K× was used for SEM imaging. AFM measurements were acquired using a Bruker Dimension FastScan AFM with NanoScope V controller, NanoScope control software (version 8.15) and ScanAsyst Air cantilevers. The peak-force tapping imaging mode was used with the scan rate and set point controlled manually, while the feedback gains and Z-limit were automatically adjusted to optimize image quality and the data was analyzed using the NanoScope Analysis software (version 1.4).

Conflict of Interest: The authors declare no competing financial interest.

Supporting Information Available: Supporting absorbance spectra, AFM statistics, Raman characterization, and TEM data. This material is available free of charge via the Internet at http://pubs.acs.org.

Acknowledgment. We thank Unidym for providing DWCNT material. K.E.M acknowledges the Karlsruhe House of Young Scientists, the Playford Memorial Trust, and the Australian Microscopy and Microanalysis Research Facility (AMMRF). We are grateful to the Karlsruhe Nano Micro Facility (KNMF) for access to the TEM facilities. This research was also supported by the Bundesministerium fur Bildung und Forschung (BMBF) as administered by POF-NanoMicro. B.S.F. gratefully acknowledges support from the Deutsche Forschungsgemeinschaft's Emmy Noether Program under Grant No. FL 834/1-1.

REFERENCES AND NOTES

1. Brozena, A. H.; Moskowitz, J.; Shao, B.; Deng, S.; Liao, H.; Gaskell, K. J.; Wang, Y. Outer Wall Selectively Oxidized, Water-Soluble Double-Walled Carbon Nanotubes. *J. Am. Chem. Soc.* **2010**, *132*, 3932–3938.
2. Piao, Y.; Chen, C.-F.; Green, A. A.; Kwon, H.; Hersam, M. C.; Lee, C. S.; Schatz, G. C.; Wang, Y. Optical and Electrical Properties of Inner Tubes in Outer Wall-Selectively Functionalized Double-Wall Carbon Nanotubes. *J. Phys. Chem. Lett.* **2011**, *2*, 1577–1582.
3. Huang, J.; Ng, A. L.; Piao, Y.; Chen, C.-F.; Green, A. A.; Sun, C.-F.; Hersam, M. C.; Lee, C. S.; Wang, Y. Covalently Functionalized Double-Walled Carbon Nanotubes Combine High Sensitivity and Selectivity in the Electrical Detection of Small Molecules. *J. Am. Chem. Soc.* **2013**, *135*, 2306–2312.
4. Okada, S.; Oshiyama, A. Curvature-Induced Metallization of Double-Walled Semiconducting Zigzag Carbon Nanotubes. *Phys. Rev. Lett.* **2003**, *91*, 216801.
5. Moradian, R.; Azadi, S.; Refii-tabar, H. When Double-Wall Carbon Nanotubes Can Become Metallic or Semiconducting. *J. Phys.: Condens. Matter* **2007**, *19*, 176209.

6. Liu, K.; Wang, W.; Xu, Z.; Bai, X.; Wang, E.; Yao, Y.; Zhang, J.; Liu, Z. Chirality-Dependent Transport Properties of Double-Walled Nanotubes Measured *in Situ* on Their Field-Effect Transistors. *J. Am. Chem. Soc.* **2008**, *131*, 62–63.
7. Bouilly, D.; Cabana, J.; Meunier, F.; Desjardins-Carrière, M.; Lapointe, F.; Gagnon, P.; Larouche, F. L.; Adam, E.; Paillet, M.; Martel, R. Wall-Selective Probing of Double-Walled Carbon Nanotubes Using Covalent Functionalization. *ACS Nano* **2011**, *5*, 4927–4934.
8. Kalbac, M.; Green, A. A.; Hersam, M. C.; Kavan, L. Tuning of Sorted Double-Walled Carbon Nanotubes by Electrochemical Charging. *ACS Nano* **2010**, *4*, 459–469.
9. Green, A. A.; Hersam, M. C. Processing and Properties of Highly Enriched Double-Wall Carbon Nanotubes. *Nat. Nanotechnol.* **2009**, *4*, 64–70.
10. Huh, J. Y.; Walker, A. R. H.; Ro, H. W.; Obrzut, J.; Mansfield, E.; Geiss, R.; Fagan, J. A. Separation and Characterization of Double-Wall Carbon Nanotube Subpopulations. *J. Phys. Chem. C* **2010**, *114*, 11343–11351.
11. Green, A. A.; Hersam, M. C. Properties and Application of Double-Walled Carbon Nanotubes Sorted by Outer-Wall Electronic Type. *ACS Nano* **2011**, *5*, 1459–1467.
12. Moshammer, K.; Hennrich, F.; Kappes, M. Selective Suspension in Aqueous Sodium Dodecyl Sulfate According to Electronic Structure Type Allows Simple Separation of Metallic from Semiconducting Single-Walled Carbon Nanotubes. *Nano Res.* **2009**, *2*, 599–606.
13. Liu, H.; Nishide, D.; Tanaka, T.; Kataura, H. Large-Scale Single-Chirality Separation of Single-Wall Carbon Nanotubes by Simple Gel Chromatography. *Nat. Commun.* **2011**, *2*, 309.
14. Liu, H.; Tanaka, T.; Urabe, Y.; Kataura, H. High-Efficiency Single-Chirality Separation of Carbon Nanotubes Using Temperature-Controlled Gel Chromatography. *Nano Lett.* **2013**, *13*, 1996–2003.
15. Tvrdy, K.; Jain, R. M.; Han, R.; Hilmer, A. J.; McNicholas, T. P.; Strano, M. S. A Kinetic Model for the Deterministic Prediction of Gel-Based Single-Chirality Single-Walled Carbon Nanotube Separation. *ACS Nano* **2013**, *7*, 1779–1789.
16. Jain, R. M.; Tvrdy, K.; Han, R.; Ulissi, Z.; Strano, M. S. Quantitative Theory of Adsorptive Separation for the Electronic Sorting of Single-Walled Carbon Nanotubes. *ACS Nano* **2014**, *8*, 3367–3379.
17. Flavel, B. S.; Kappes, M. M.; Krupke, R.; Hennrich, F. Separation of Single-Walled Carbon Nanotubes by 1-Dodecanol-Mediated Size-Exclusion Chromatography. *ACS Nano* **2013**, *7*, 3557–3564.
18. Flavel, B. S.; Moore, K. E.; Pfohl, M.; Kappes, M. M.; Hennrich, F. Separation of Single-Walled Carbon Nanotubes with a Gel Permeation Chromatography System. *ACS Nano* **2014**, *8*, 1817–1826.
19. Moore, K. E.; Pfohl, M.; Hennrich, F.; Chakradhanula, V. S.; Kuebel, C.; Kappes, M. M.; Shapter, J. G.; Krupke, R.; Flavel, B. S. Separation of Double-Walled Carbon Nanotubes by Size Exclusion Column Chromatography. *ACS Nano* **2014**, *8*, 6756–64.
20. Miyata, Y.; Shiozawa, K.; Asada, Y.; Ohno, Y.; Kitaura, R.; Mizutani, T.; Shinohara, H. Length-Sorted Semiconducting Carbon Nanotubes for High-Mobility Thin Film Transistors. *Nano Res.* **2011**, *4*, 963–970.
21. Wu, J.; Xie, L.; Hong, G.; Lim, H.; Thendie, B.; Miyata, Y.; Shinohara, H.; Dai, H. Short Channel Field-Effect Transistors from Highly Enriched Semiconducting Carbon Nanotubes. *Nano Res.* **2012**, *5*, 388–394.
22. Zhang, J.; Gui, H.; Liu, B.; Liu, J.; Zhou, C. Comparative Study of Gel-Based Separated Arcdischarge, Hipco, and Comocat Carbon Nanotubes for Macroelectronic Applications. *Nano Res.* **2013**, *6*, 906–920.
23. Araujo, P. T.; Doorn, S. K.; Kilina, S.; Tretiak, S.; Einarsson, E.; Maruyama, S.; Chacham, H.; Pimenta, M. A.; Jorio, A. Third and Fourth Optical Transitions in Semiconducting Carbon Nanotubes. *Phys. Rev. Lett.* **2007**, *98*, 067401.
24. Bachilo, S. M.; Strano, M. S.; Kittrell, C.; Hauge, R. H.; Smalley, R. E.; Weisman, R. B. Structure-Assigned Optical Spectra of Single-Walled Carbon Nanotubes. *Science* **2002**, *298*, 2361–2366.
25. Charlier, J. C.; Michenaud, J. P. Energetics of Multilayered Carbon Tubules. *Phys. Rev. Lett.* **1993**, *70*, 1858–1861.
26. Blanch, A. J.; Quinton, J. S.; Shapter, J. G. The Role of Sodium Dodecyl Sulfate Concentration in the Separation of Carbon Nanotubes Using Gel Chromatography. *Carbon* **2013**, *60*, 471–480.
27. Wallace, E. J.; Sansom, M. S. Carbon Nanotube Self-Assembly with Lipids and Detergent: A Molecular Dynamics Study. *Nanotechnology* **2009**, *20*, 045101.
28. Xu, Z.; Yang, X.; Yang, Z. A Molecular Simulation Probing of Structure and Interaction for Supramolecular Sodium Dodecyl Sulfate/Single-Wall Carbon Nanotube Assemblies. *Nano Lett.* **2010**, *10*, 985–991.
29. Duan, W. H.; Wang, Q.; Collins, F. Dispersion of Carbon Nanotubes with Sds Surfactants: A Study from a Binding Energy Perspective. *Chem. Sci.* **2011**, *2*, 1407–1413.
30. Tummala, N. R.; Striolo, A. Sds Surfactants on Carbon Nanotubes: Aggregate Morphology. *ACS Nano* **2009**, *3*, 595–602.
31. Niyogi, S.; Densmore, C. G.; Doorn, S. K. Electrolyte Tuning of Surfactant Interfacial Behavior for Enhanced Density-Based Separations of Single-Walled Carbon Nanotubes. *J. Am. Chem. Soc.* **2008**, *131*, 1144–1153.
32. Jain, R. M.; Howden, R.; Tvrdy, K.; Shimizu, S.; Hilmer, A. J.; McNicholas, T. P.; Gleason, K. K.; Strano, M. S. Polymer-Free Near-Infrared Photovoltaics with Single Chirality (6,5) Semiconducting Carbon Nanotube Active Layers. *Adv. Mater.* **2012**, *24*, 4436–4439.
33. Kominkova, Z.; Vales, V.; Hersam, M. C.; Kalbac, M. Towards Quantification of the Ratio of the Single and Double Wall Carbon Nanotubes in Their Mixtures: An *in Situ* Raman Spectroelectrochemical Study. *Carbon* **2014**, *78*, 366–373.
34. Arnold, M. S.; Stupp, S. I.; Hersam, M. C. Enrichment of Single-Walled Carbon Nanotubes by Diameter in Density Gradients. *Nano Lett.* **2005**, *5*, 713–718.
35. Arnold, M. S.; Green, A. A.; Hulvat, J. F.; Stupp, S. I.; Hersam, M. C. Sorting Carbon Nanotubes by Electronic Structure Using Density Differentiation. *Nat. Nanotechnol.* **2006**, *1*, 60–65.
36. Kim, W.-J.; Nair, N.; Lee, C. Y.; Strano, M. S. Covalent Functionalization of Single-Walled Carbon Nanotubes Alters Their Densities Allowing Electronic and Other Types of Separation. *J. Phys. Chem. C* **2008**, *112*, 7326–7331.
37. Ghosh, S.; Bachilo, S. M.; Weisman, R. B. Advanced Sorting of Single-Walled Carbon Nanotubes by Nonlinear Density-Gradient Ultracentrifugation. *Nat. Nanotechnol.* **2010**, *5*, 443–450.
38. Wang, F.; Dukovic, G.; Brus, L. E.; Heinz, T. F. The Optical Resonances in Carbon Nanotubes Arise from Excitons. *Science* **2005**, *308*, 838–841.
39. Ando, T. Excitons in Carbon Nanotubes. *J. Phys. Soc. Jpn.* **1997**, *66*, 1066–1073.
40. Ichida, M.; Mizuno, S.; Saito, Y.; Kataura, H.; Achiba, Y.; Nakamura, A. Coulomb Effects on the Fundamental Optical Transition in Semiconducting Single-Walled Carbon Nanotubes: Divergent Behavior in the Small-Diameter Limit. *Phys. Rev. B* **2002**, *65*, 241407.
41. Krupke, R.; Hennrich, F.; Weber, H. B.; Kappes, M. M. v. Löhneysen, H., Simultaneous Deposition of Metallic Bundles of Single-Walled Carbon Nanotubes Using Ac-Dielectrophoresis. *Nano Lett.* **2003**, *3*, 1019–1023.
42. Krupke, R.; Hennrich, F.; Weber, H. B.; Beckmann, D.; Hampe, O.; Malik, S.; Kappes, M. M.; v. Löhneysen, H. Contacting Single Bundles of Carbon Nanotubes with Alternating Electric Fields. *Appl. Phys. A: Mater. Sci. Process.* **2003**, *76*, 397–400.
43. Chung, J.; Lee, K.-H.; Lee, J.; Ruoff, R. S. Toward Large-Scale Integration of Carbon Nanotubes. *Langmuir* **2004**, *20*, 3011–3017.
44. Vijayaraghavan, A.; Marquardt, C. W.; Dehm, S.; Hennrich, F.; Krupke, R. Imaging Defects and Junctions in Single-Walled Carbon Nanotubes by Voltage-Contrast Scanning Electron Microscopy. *Carbon* **2010**, *48*, 494–500.
45. Steiner, M.; Engel, M.; Lin, Y.-M.; Wu, Y.; Jenkins, K.; Farmer, D. B.; Humes, J. J.; Yoder, N. L.; Seo, J.-W. T.; Green, A. A.; et al. High-Frequency Performance of Scaled Carbon Nanotube Array Field-Effect Transistors. *Appl. Phys. Lett.* **2012**, *101*, 053123.